
Research Article: New Research | Development

SRF is required for maintenance of astrocytes in non-reactive state in the mammalian brain

<https://doi.org/10.1523/ENEURO.0447-19.2020>

Cite as: eNeuro 2021; 10.1523/ENEURO.0447-19.2020

Received: 28 October 2019

Revised: 24 December 2020

Accepted: 24 December 2020

This Early Release article has been peer-reviewed and accepted, but has not been through the composition and copyediting processes. The final version may differ slightly in style or formatting and will contain links to any extended data.

Alerts: Sign up at www.eneuro.org/alerts to receive customized email alerts when the fully formatted version of this article is published.

Copyright © 2021 Jain et al.

This is an open-access article distributed under the terms of the Creative Commons Attribution 4.0 International license, which permits unrestricted use, distribution and reproduction in any medium provided that the original work is properly attributed.

Manuscript Title Page Instructions

1
2
3
4
5
6
7
8
9
10
11
12
13
14
15
16
17
18
19
20
21
22
23
24
25
26
27
28
29
30
31
32
33
34
35
36
37
38
39
40
41
42
43
44

Please list the following information on your separate title page in Word .DOC format in the order listed below and upload as a Title Page file at submission

1. Manuscript Title (50 word maximum)

SRF is required for maintenance of astrocytes in non-reactive state in the mammalian brain

2. Abbreviated Title (50 character maximum)

Mechanism regulating reactive astrogliosis

3. List all Author Names and Affiliations in order as they would appear in the published article

Monika Jain¹, Soumen Das¹, Paul P. Y. Lu², Garima Virmani¹, Sumitha Soman¹, Surya Chandra Rao Thumu¹, David H. Gutmann³ and Narendrakumar Ramanan^{1*}

¹Centre for Neuroscience, Indian Institute of Science, Bangalore 560012, Karnataka, India

²Jiangsu Hengrui Medicine, Cambridge, MA 02139, USA

³Department of Neurology, Washington University School of Medicine, St. Louis, MO 63110, USA

4. Author Contributions:

N.R. conceived of the project and designed the experiments. M.J. performed the experiments and analyzed the data. S.D and G.V. helped with quantification, S.S. helped with quantitative PCR, P.P.Y.L generated the *Srf* mutant mice and carried out the initial characterization. S.C.R.T. helped with BBB experiments and D.H.G. shared valuable reagents. N.R. wrote the manuscript and all authors reviewed and edited the manuscript.

5. Correspondence should be addressed to (include email address)

Narendrakumar Ramanan: naren@iisc.ac.in

6. Number of Figures: 08

7. Number of Tables: 0

8. Number of Multimedia: 0

9. Number of words for Abstract: 224

10. Number of words for Significance

Statement: 101

11. Number of words for Introduction: 429

12. Number of words for Discussion: 1313

50 **13. Acknowledgements**

51

52 We thank Ramanan lab members for critical comments on the manuscript. Dr. Deepak
53 Nair for help with quantification of BBB experiment. The Microscopy facility and the Central
54 Animal Facility in the Division of Biological Sciences for confocal imaging and animal care
55 respectively.

56

57

58 **14. Conflict of Interest**

59

60 **A. No (State 'Authors report no conflict**
61 **of interest')**

62 Authors report no conflict of interest.

63

64 **B. Yes (Please explain)**

65

66

67 **15. Funding sources**

68

69 SwarnaJayanti Fellowship (DST/SJF/LSA-01/2012-2013), Department of Science and
70 Technology, India (N.R.), Department of Biotechnology (DBT) grant,
71 (BT/PR26216/GET/119/234/2017) (N.R.), DBT-IISc Partnership Program grant (N.R). M.J.
72 and S.D. were supported by a senior research fellowship from the University Grants
73 Commission, India. G.V. was supported by a senior research fellowship from the Council for
74 Scientific and Industrial Research, India. S.C.R.T. was supported by postdoctoral fellowship
75 (PDF/2017/001385) from the Department of Science and Technology, India.

76

77

78 **SRF is required for maintenance of astrocytes in non-reactive state in the mammalian**

79 **brain**

80

81 **ABSTRACT**

82 Astrocytes play several critical roles in the normal functioning of the mammalian brain including
83 ion homeostasis, synapse formation and synaptic plasticity. Following injury and infection or in
84 the setting of neurodegeneration, astrocytes become hypertrophic and reactive, a process termed
85 astrogliosis. Although acute reactive gliosis is beneficial in limiting further tissue damage,
86 chronic gliosis becomes detrimental for neuronal recovery and regeneration. Several
87 extracellular factors have been identified that generate reactive astrocytes; however, very little is
88 known about the cell-autonomous transcriptional mechanisms that regulate the maintenance of
89 astrocytes in the normal non-reactive state. Herein, we show that conditional deletion of the
90 stimulus-dependent transcription factor, serum response factor (SRF) in astrocytes (*Srf*^{GFAP}-
91 CKO) results in astrogliosis marked by hypertrophic morphology and increased expression of
92 GFAP, vimentin and nestin. These reactive astrocytes were not restricted to any specific brain
93 region and were seen in both white and grey matter in the entire brain. This astrogliosis persisted
94 throughout adulthood concomitant with microglial activation. Importantly, the *Srf* mutant mouse
95 brain did not exhibit any cell death or blood brain barrier (BBB) deficits suggesting that
96 apoptosis and leaky BBB are not the causes for the reactive phenotype. The mutant astrocytes
97 expressed more A2 reactive astrocyte marker genes and the *Srf*^{GFAP}CKO mice exhibited normal
98 neuronal numbers indicating that SRF-deficient gliosis astrocytes are not neurotoxic. Together
99 our findings suggest that SRF plays a critical role in astrocytes to maintain them in a non-
100 reactive state.

101

102 **SIGNIFICANCE STATEMENT**

103 In response to CNS injury, infection and in neurodegeneration, astrocytes undergo complex
104 structural and physiological changes termed as reactive gliosis. Currently, the molecular
105 mechanisms that regulate the non-reactive state of the astrocytes are poorly understood. We
106 report that the SRF transcription factor is required for the maintenance of astrocytes in the non-
107 reactive state such that its conditional deletion in astrocytes results in widespread reactive
108 astrogliosis. The SRF-deficient reactive astrocytes are persistent, non-proliferating and are not
109 caused by cell death or impaired blood brain barrier integrity. In this regard, SRF regulates
110 reactive astrocyte generation in the mammalian brain in a cell-autonomous manner.

111

112 **INTRODUCTION**

113 As an essential part of the central nervous system (CNS), astrocytes play critical roles in
114 nearly every facet of its development and function including ion and neurotransmitter
115 homeostasis, maintenance of the blood brain barrier (BBB), synapse formation and elimination,
116 and synaptic transmission (Barres, 2008; Kimelberg, 2010; Kimelberg and Nedergaard, 2010).
117 In addition, astrocytic dysfunction are central in several CNS disorders such as epilepsy,
118 amyotrophic lateral sclerosis and Alzheimer's disease (Seifert et al., 2006; Phatnani and
119 Maniatis, 2015). In response to CNS injuries and pathologies, astrocytes undergo a spectrum of
120 gene expression as well as physiological and structural changes, a process known as reactive
121 astrogliosis (Burda and Sofroniew, 2014; Liddelow and Barres, 2017). These astrocytic
122 responses depend on the severity of the CNS trauma and can range from transient responses
123 lasting a few days to a more permanent glial scar formation (Sofroniew, 2009, 2015).

124

125 Reactive astrogliosis is largely considered beneficial to the CNS, where reactive
126 astrocytes provide protection by several mechanisms, ranging from efficient uptake of
127 excitotoxic glutamate, preventing oxidative stress and reducing edema, to restricting
128 inflammation, facilitating blood brain barrier repair and restricting spread of infection (Hamby
129 2010; Escartin 2008; Pekny 2014). However, astrogliosis can also cause detrimental effects
130 wherein reactive astrocytes inhibit CNS regenerative responses, contribute to
131 neuroinflammation, generate reactive oxygen species and cause cell death (Pekny 2014;
132 Sofroniew 2014). Previous studies have identified several extracellular factors and intracellular
133 signaling pathways that regulate different aspects of astrogliosis including cytokines, growth
134 factors, purines, Endothelin-1, BMP receptors, Eph4 and Aquaporin 4 (Correa-Cerro and
135 Mandell, 2007; Kang and Hebert, 2011; Sofroniew, 2014).

136

137 Currently, we know little about the identities of transcription factors that are necessary to
138 maintain astrocytes in a non-reactive state. SRF is a stimulus-dependent transcription factor
139 important for several aspects of nervous system development (Knoll and Nordheim, 2009). SRF
140 has been shown to play a critical role in oligodendrocyte and astrocyte development (Stritt et al.,
141 2009; Lu and Ramanan, 2012) but its functions in astrocytes remain unknown. In this study, we
142 conditionally ablated SRF in astrocytes using a GFAP-Cre transgenic line (Bajenaru et al., 2002).
143 The brains of *Srf*^{GFAP}CKO mice exhibited reactive astrogliosis starting 3 weeks of age. These
144 reactive astrocytes were not restricted to any specific region and were seen throughout the brain.
145 The reactive gliosis persisted throughout adulthood with concomitant microglial activation. We
146 did not observe any changes in cell death or blood brain barrier integrity, indicating that these

147 extrinsic factors are unlikely the cause of gliosis. Together our findings suggest that SRF is a
148 critical cell autonomous regulator of non-reactive state of astrocytes throughout the brain.

149

150 **Materials and Methods**

151 **Animals.** *Srf*-floxed mice were obtained from Jackson laboratories (Stock No 006658). These
152 mice were bred with hGFAP-Cre (generously provided by Dr. David Gutmann, Washington
153 University School of Medicine, St. Louis, MO) to obtain *Srf*^{f/f}-GFAPCre^{+/-} (*Srf*^{GFAP}CKO). *Srf*^{f/f}
154 mice served as control in all experiments. Both male and female mice were used in all the
155 experiments. All experiments were conducted in accordance with the animal care standards and
156 use and approved by the Institutional Animal Ethics Committee. Control and mutant mice were
157 housed together, and cage mates were randomly assigned to experimental groups. All
158 experiments were conducted blinded to the genotype of the mice used.

159

160 **Immunohistochemistry.** Mice were fixed by transcardial perfusion using 4% PFA. The brains
161 were cryoprotected in 30% sucrose, frozen and stored in -80° C until further use. For staining,
162 30 µm thick cryosections were incubated in blocking/permeabilization solution containing 0.3%
163 Triton-X and 3% goat serum in PBS (pH 7.4) for 1 hour followed by overnight incubation in
164 primary antibody. The brain sections were then washed in PBS and incubated in secondary
165 antibody for 1 hour. The sections were finally mounted in DAPI-containing mounting medium
166 (Vector Laboratories). For SRF immunostaining, heat-induced epitope retrieval was carried out
167 by incubating the sections in 10 mM sodium citrate, pH 8.9 for 30 min at 95 °C. The following
168 primary antibodies were used: anti-GFAP (1:1000; Sigma-Aldrich Cat# G3893,
169 RRID:AB_477010), anti-GFAP (1:1000; Agilent Cat# Z0334, RRID:AB_10013382), anti-Nestin

170 (1:1000; Millipore Cat# MAB5326, RRID:AB_2251134), anti-Vimentin (1:50; DSHB Cat# 40E-
171 C, RRID:AB_528504), anti-S100 β (1:1000; Sigma-Aldrich Cat# S2644, RRID:AB_477501),
172 anti-S100 β (1:500; Synaptic systems Cat# 287006, RRID:AB_2713986), anti-Aldh1L1 (1:100;
173 UC Davis/NIH NeuroMab Facility Cat# 73-140, RRID:AB_10673447), anti-Iba1 (1:1000; Wako
174 Cat# 019-19741, RRID:AB_839504), anti-PhosphoHistoneH3 (1:500; Sigma-Aldrich Cat#
175 H0412, RRID:AB_477043), anti-Caspase 3 active (1:1500, Millipore Cat# 04-439,
176 RRID:AB_673061), anti-SRF (1:200; Santa Cruz Biotechnology Cat# sc-335,
177 RRID:AB_2255249) and anti-NeuN (1:500; Millipore Cat# MAB377, RRID:AB_2298772).
178 The following secondary antibodies were, AlexaFluor-488, -594, and -647 conjugated anti-
179 rabbit, anti-chicken, and anti-mouse at 1:1000 dilution (Life Technologies). Biotinylated anti-
180 mouse and anti-rabbit secondary antibodies (1:250; Vector Laboratories) were used along with
181 Vectastain ABC Elite, ImmPACT VIP substrate and ImmPACT DAB substrate kits (Vector
182 Labs). All the images were captured using conventional fluorescence microscopy (Eclipse 80i,
183 Nikon), except the images for SRF immunostaining and BBB measurement, which were
184 captured using a confocal microscope (LSM 880, Zeiss).

185

186 **RNA Isolation and quantitative realtime PCR.** Total RNA was isolated from forebrain of 3-5
187 wk old control and *Srf*^{GFAP}CKO mice using the PureLink™ RNA Mini Kit (Thermo Fisher
188 Scientific) as per the manufacturer's protocol. 2 μ g of total RNA was used for first-strand cDNA
189 synthesis using the first strand synthesis kit (Invitrogen Inc.). Quantitative RT-PCR was done
190 with 100 ng of cDNA and KAPA SYBR FAST ABI prism kit (Cat. No. KK4604) using the
191 following program: 95° C for 3 min followed by 39 cycles of 95° C for 5 sec, 55° C for 30 sec and
192 72° C for 40 sec. The PCR reaction was carried out in QuantStudio 7 Flex Real-Time PCR

193 System (Invitrogen Biosciences). The primers used were: *Srf*, Fwd, 5'-
194 ACCAGTGTCTGCTAGTGTCAGC-3' and Rev, 5'-CATGGGGACTAGGGTACATCAT-3';
195 *Rps29*, Fwd 5'-CCAGCAGCTCTACTGGAGTCA-3' and Rev, 5'-
196 AGACTAGCATGATCGGTTCCA-3'. *Il1 β* , Fwd, 5'-ATCAACAAGCAATTCCTCGATGA-3'
197 and Rev, 5'-CAGCATTCGCTTCAAGGACATA-3'; TNFa, Fwd, 5'-
198 CCCTCACACTCAGATCATCTTCT-3' and Rev, 5'-GCTACGACGTGGGCTACAG-3'; *Ccl2*,
199 Fwd, 5'-TTAAAAACCTGGATCGGAACCAA-3' and Rev, 5'-
200 GCATTAGCTTCAGATTTACGGGT-3'. Expression of *Srf* and other genes were normalized to
201 that of the housekeeping gene, *Rps29*. The primers for A1, A2 and pan-reactive astrocytes were
202 from a previously published study (Liddelow et al., 2017).

203

204 **BBB permeability assay.** Two assays were used as previously described (Andreone et al.,
205 2017) to measure the integrity of BBB using 6-mon old *Srf*^{GFAP}CKO mice. In the first assay,
206 mice were deeply anesthetized with isoflurane and injected with 20 μ l of 10 kDa dextran
207 fluorescein (10 mg/ml, Invitrogen; D1820) into the left ventricle of the heart, and allowed to
208 circulate for 5 min. Their brains were collected and post-fixed in 4% PFA overnight, frozen and
209 stored at -80 $^{\circ}$ C. 30 μ m thick cryosections were mounted using mounting media supplemented
210 with DAPI (Vector Labs, USA) and analyzed using a confocal microscope (LSM 880, Zeiss). In
211 the second assay, 10 μ l of HRP Type II (5mg/ml) was administered transcidentally and allowed to
212 circulate for 5 min. The brains were collected and immersed in 2% glutaraldehyde in 4% PFA in
213 cacodylate buffer (0.1M, pH 7.3) at RT for 1 hour. The brains were then shifted to 4 $^{\circ}$ C
214 overnight and sectioned at 100 μ m using a Leica vibratome, and processed using ImmPACT VIP
215 kit (Vector Labs). For quantification of dextran fluorescein injection, epifluorescence images

216 (63X) of brain sections were analyzed using ImageJ. Brain sections from the same rostro-caudal
217 position were analyzed. At least 12 different regions were taken and the ratio of the fluorescence
218 or color intensity (outside versus inside the vessel) was measured.

219

220 **Quantification of fluorescence intensity and cell numbers.** For measuring fluorescence
221 intensity, images were scaled for 10X magnification and normalized to the same exposure time.
222 Ten to twelve areas of field (ROI, 500x500 μm^2) in the same rostro-caudal axis were drawn per
223 image, and the intensities were measured using ImageJ (Fiji) after subtracting the background
224 fluorescence from both control and knockout sections. For the hippocampus, cell numbers or
225 fluorescence intensities were measured in the *stratum oriens* and *stratum radiatum*. For cell
226 counts, images were taken at 4X magnification. Four ROIs of 1200x1200 μm^2 (1 mm^2 for
227 hippocampal CA1 and CA3) in the same rostro-caudal axis were drawn per image, and the
228 number of cells per ROI were counted with cell counter plugin using ImageJ (Fiji). For SRF
229 fluorescence intensity, the SRF fluorescence signal within the DAPI area was quantified using
230 ImageJ.

231

232 **Quantification of microglial activation.** Brain sections from *Srf*^{GFAP}CKO mice and control
233 littermates at different ages (3 wk, 3 mon and 12 mon) were fluorescently immunostained for
234 Iba1. At least five different cortical regions in the same rostro-caudal axis were taken in all the
235 mice to measure fluorescence intensity. This was then compared between the control and the
236 knockout mice to get the fold difference in fluorescence. ImageJ was used to measure the
237 percentage increase in fluorescence per unit field and this was compared between control and

238 knockout groups at all the experimental time points as mentioned in statistical analysis. The area
239 of the field was 500x500 μm^2 .

240

241 **TUNEL assay.** The TUNEL assay was carried out using Click-IT Plus TUNEL assay kit
242 (Molecular Probes, Thermo Fisher Scientific) according to the manufacturer's instructions.
243 Briefly, brains fixed in 4% PFA and 30 μm cryosections were permeabilized with proteinase K
244 solution for 15 min and then incubated with TdT reaction mixture for 60 min at 37° C and
245 subsequently with EdUTP for 30 min. The detection was achieved through click reaction
246 between the dUTP bound alkyne group and a picolyl azide fluorescent dye for 30 min. The slides
247 were washed with 3% BSA in PBS for 5 min and rinsed in 1X PBS. The slides were mounted
248 using mounting medium containing DAPI (Vector Labs) and observed using an epifluorescence
249 microscope (Eclipse 80i, Nikon) using appropriate filters and captured using Metamorph
250 software. Numbers of TUNEL⁺ cells in the CA1, CA3 and DG regions of entire rostral to caudal
251 brain regions were counted using Image J software. The area of the field for counting the number
252 of TUNEL⁺ cells was 250x250 μm^2 .

253

254 **Statistical analyses.** Analyses were done using GraphPad Prism 6. The comparisons between
255 two groups was done using unpaired two-tailed Student's *t*-test. All the statistical details for each
256 experiment, including the n value, the statistical test used, P value, significance of comparisons is
257 mentioned in the figure legends.

258

259

260 **RESULTS**

261 ***Srf* deletion in astrocytes results in reactive astrogliosis**

262 To study the function of SRF in astrocytes, we generated *Srf*^{GFAP}CKO conditional
263 knockout mice using a hGFAP-Cre transgenic mouse line, in which Cre expression was found to
264 occur predominantly in astroglial progenitor cells starting at embryonic day 16.5 (E16.5)
265 (Bajenaru et al., 2002). *Srf*^{GFAP}CKO mice were obtained in normal Mendelian ratio, appeared
266 normal at birth and did not exhibit any gross morphological deficits such as neocortical
267 lamination and hippocampal architecture (data not shown). We first confirmed *Srf* deletion in
268 astrocytes. Co-immunostaining for SRF, S100 β and NeuN revealed robust SRF expression in
269 both the astrocytes and neurons in 3-5 wk old control mice (Fig 1A). In the brain sections of
270 *Srf*^{GFAP}CKO mutant mice, there was robust SRF expression in neurons while it was absent in the
271 astrocytes (Fig. 1 A, B). We observed that the antigen retrieval method caused a slightly
272 punctate SRF immunostaining, which was more pronounced in the mutant sections. However,
273 this pattern of staining overlapped with NeuN but not with S100 β in the mutant sections (Fig.
274 1A). Quantitative and semi-quantitative real time PCR using total RNA isolated from whole
275 brain showed decreased *Srf* expression in mutants relative to controls (Fig. 1C, D).

276

277 We then asked whether *Srf* deletion had any effect on astrocyte development. In 3-5 wk
278 old control mice, astrocytes in hippocampus and fibrous astrocytes in the white matter expressed
279 GFAP, while there was no detectable GFAP expression in the neocortical astrocytes, which have
280 been shown to downregulate GFAP expression postnatally (Buffo et al., 2008; Robel et al., 2009)
281 (Fig. 2A ,B). However, the astrocytes in control mice expressed other astrocytic markers, such
282 as S100 β (Fig. 2C). In striking contrast, astrocytes in the *Srf*^{GFAP}CKO mice exhibited
283 pronounced GFAP expression (Fig. 2A, B) along with hypertrophic morphology as seen from

284 immunostaining for GFAP, Aldh1L1 and S100 β (Fig. 2A-C), both hallmarks of reactive
285 astrogliosis. Cell counts of S100 β -positive cells revealed no change in the number of astrocytes
286 between control and mutant mice in all regions analyzed (Fig. 2D). We had shown earlier that
287 neuron-specific deletion of SRF does not affect astrocyte differentiation or cause reactive gliosis
288 (Lu and Ramanan, 2012). Therefore, although unlikely, any transient Cre expression in neurons
289 by the hGFAP-Cre transgene is unlikely to cause the gliosis phenotype seen in *Srf*^{GFAPCKO}
290 mice.

291

292 Astrocytes exhibit regional heterogeneity and previous gene deletion studies have shown
293 region-specific generation of reactive astrocytes (Garcia et al., 2010; Kang et al., 2014b). We
294 therefore asked whether reactive astrocytes in *Srf*^{GFAP}CKO mice were also regionally restricted.
295 For this, we analyzed serial sections from the entire brain of control and *Srf* knockout mice. We
296 found that astrocytes in most regions of the brain in control mice did not express or weakly
297 expressed GFAP (Fig. 2A, B). In striking contrast, brain sections from *Srf*^{GFAP}CKO mice
298 exhibited intense GFAP expression in all brain regions analyzed including in striatum and corpus
299 callosum (data not shown). To further confirm that the astrocytes in *Srf*^{GFAP}CKO mice are
300 indeed reactive, we immunostained for known astrogliosis markers, vimentin and nestin (Ridet et
301 al., 1997). In contrast to control littermates, the *Srf*^{GFAP}CKO mice exhibited robust nestin-
302 positive (Fig. 3A, B) and vimentin-positive (Fig. 3C, D) astrocytes, thus confirming their
303 reactive state. These observations suggest that astrocyte-specific deletion of *Srf* results in
304 reactive astrocytes.

305

306 **Astrogliosis seen in *Srf* knockout mice is not induced by cell death.**

307 Astrogliosis is generally induced by several extrinsic factors, such as cell death or a leaky
308 blood brain barrier (BBB) (Pekny and Nilsson, 2005). We first analyzed cell death by
309 immunostaining for cleaved caspase-3 as well as by TUNEL staining. We did not observe any
310 discernible cell death at 2 weeks of age in *Srf*^{GFAP}CKO mice, just prior to the onset of
311 astrogliosis (Fig. 4A-C). This strongly suggested that reactive astrogliosis seen in the *Srf*
312 knockout mice is not triggered by cell death. During conditions of severe neural injury or
313 trauma, reactive astrocyte undergo proliferation (Sofroniew, 2014). To determine whether SRF-
314 deficient reactive astrocytes are proliferating, brain sections from *Srf*^{GFAP}CKO mice and control
315 littermates were immunostained with the proliferation marker, phosphoHistone-H3 (pH3).
316 There were no phosphoHistone-H3-positive cells observed in either *Srf* mutant mice or their
317 control littermates, excluding the presence of proliferating astrocytes (Fig. 4D).

318

319 **Blood brain barrier is unaffected in *Srf* knockout mice**

320 Given the widespread and persistent reactive astrogliosis seen in *Srf* mutant mice, it is
321 possible that a leaky blood brain barrier (BBB) could be the likely cause for the astrogliosis
322 observed in *Srf* knockout mice (Pekny and Nilsson, 2005). To study BBB integrity, we injected
323 two different tracers, 10 kDa dextran fluorescein (Fig. 5A, B, C) and 44 kDa HRP type II (Fig.
324 5A, D, E), into 3-5 week old *Srf*^{GFAP}CKO mutant and control mice (Andreone et al., 2017). We
325 did not observe any discernible presence of these tracers in the brain parenchyma of *Srf* knockout
326 mice relative to their littermate controls (Fig. 5), supporting an intact BBB.

327

328 **Persistent reactive astrogliosis seen in *Srf*^{GFAP}CKO mice throughout adulthood**

329 Astrogliosis could be a transient phenomenon, lasting a few days to several weeks, or a
330 long-lasting event resulting in a glial scar, depending on the severity of trauma or injury
331 (Sofroniew, 2014). We therefore asked whether the astrogliosis seen in *Srf*^{GFAP}CKO mice is a
332 transient process. To address this, we immunostained brain sections from 3-month and 12-
333 month old control and knockout mice. The astrocytes in hippocampus of control mice showed
334 normal GFAP expression while there was very faint or no GFAP expression in the astrocytes in
335 the other brain regions both at either 3 month (Fig. 6A, B) or 12 months of age (Fig. 6C, D). In
336 contrast, the astrocytes in the knockout mice, at both 3 and 12 months of age, expressed intense
337 GFAP expression and exhibited hypertrophy in all brain regions (Fig. 6A-D) similar to that seen
338 at 3 weeks (Fig. 2, 3). To further confirm astrogliosis, we immunostained for vimentin and
339 found robust expression only in the astrocytes in the knockout mice but not in their control
340 littermates (Fig. 6E-G). Immunostaining for phosphoHistone-H3 did not reveal any positive
341 cells, suggesting that these astrocytes are also not proliferative in older mice (Fig. 6H). Together
342 these observations demonstrate that SRF ablation in astrocytes results in widespread astrogliosis
343 that persists through adulthood.

344

345 **Microglial activation in *Srf*^{GFAP}CKO mice**

346 Reactive astrocytes are often observed along with microgliosis (Frank and Wolburg,
347 1996; Zhang et al., 2010). We therefore asked whether microglia exhibited a reactive state in the
348 *Srf* knockout mice. Immunostaining for the microglial marker, Iba1 showed increased
349 expression in brain sections from 3-wk old mutant mice, relative to control littermates, indicative
350 of reactive microglia (Fig. 7A, B). We then quantified the number of Iba1⁺ cells and found no
351 significant difference in microglial numbers between control and knockout mice (Fig. 7C).

352 However, we noticed that the microglia tend to form clusters in the cortex and hippocampus
353 (Fig. 7A). We next asked whether microgliosis also persisted throughout adulthood similar to
354 that seen for astrogliosis. As seen at 3 weeks, brain sections from 3-month and 12-month old
355 *Srf*^{GFAP}CKO mice also showed strong upregulation of Iba1 expression relative to that from
356 control mice (Fig. 7D, E) suggesting that microglia also exhibited a reactive state along with
357 reactive astrocytes. Similar to that seen at 3 wks of age, we did not find any difference in the
358 number of Iba1⁺ cells in both 3-mon and 12-mon old *Srf*^{GFAP}CKO mice compared to control
359 littermates (Fig. 7F, G). Immunostaining for proliferation marker, phosphoHistone-H3 did not
360 reveal any positive cells (Fig. 4D, 6H) indicating that these reactive microglia are also not
361 proliferative.

362

363 **Persistent gliosis in *Srf*^{GFAP}CKO mice does not affect neuronal viability**

364 Recent studies have shown that reactive astrocytes can be broadly classified as either
365 neurotoxic (A1) or neuroprotective (A2) depending on the external stimuli (Zamanian et al.,
366 2012; Liddelow et al., 2017). In order to determine the phenotypic state of SRF-deficient
367 reactive astrocytes, we performed quantitative RT-PCR for some of the A1 (*Psm8*, *H2T23*,
368 *H2D1*, *Srgn*), A2 (*Cd109*, *Ptgs2*, *Clcf1*, *Cd14*) and pan-reactive marker genes (*Serpina3n*, *Gfap*).
369 Although we found that the *Srf*^{GFAP}CKO mice expressed both A1 and A2 genes, there were more
370 A2 reactive astrocyte marker genes that were upregulated compared to A1 genes suggesting that
371 the SRF-deficient reactive astrocytes are likely to be A2-like (Fig. 8A). Since we also observed
372 microgliosis, we next assessed the expression of neuroinflammatory genes. Quantitative PCR
373 showed a significant increase in the expression of *Il1β* and *Ccl2/Mcp-1* but not *TNFα* in the

374 brains of *Srf*^{GFAP}CKO mice (Fig. 8A) suggesting that these genes could be one of the underlying
375 causes of microgliosis observed in the *Srf* mutant mice.

376

377 We next asked whether prolonged gliosis in the SRF-GFAP mutant mice affected
378 neuronal numbers. For this, 5-wk and 12-mon old brain sections from *Srf*^{GFAP}CKO mice and
379 control littermates were immunostained for the neuronal marker, NeuN. We did not observe any
380 significant difference in NeuN-positive cells in the brains of mutant and control mice at both
381 these ages (Fig. 8B-D). This suggested that persistent gliosis observed in the brains of
382 *Srf*^{GFAP}CKO mice did not affect neuronal survival and that SRF-deficient reactive astrocytes are
383 likely not neurotoxic.

384

385 **DISCUSSION**

386 Reactive astrogliosis is an important cellular response to neuronal injury, infection and
387 neurodegeneration in the CNS, and this is critical to reduce inflammation, restrict tissue damage
388 and cell death, and promote tissue repair (Sofroniew, 2005; Pekny and Pekna, 2014). Currently,
389 very little is known about the cell-intrinsic mechanisms that regulate the conversion of an
390 astrocyte from a non-reactive to a reactive state. In this study, we show that deletion of the
391 transcription factor, SRF in astrocytes results in widespread reactive gliosis in the brain starting 3
392 weeks of age. The reactive astrocytes persisted along with microgliosis throughout adulthood
393 and both astrocytes and microglia did not exhibit proliferation. Our results suggest that SRF is
394 required in a cell-autonomous manner to regulate reactive astrogliosis in the mammalian brain.

395

396 SRF is a ubiquitously expressed transcription factor that has been shown to play critical
397 roles in several aspects of nervous system development and function (Knoll and Nordheim,
398 2009). Deletion of SRF in developing and adult neurons resulted in deficits in neuronal
399 migration, axon growth, hippocampal circuit formation, activity-dependent gene expression and
400 learning and memory (Alberti et al., 2005; Ramanan et al., 2005; Etkin et al., 2006; Knoll et al.,
401 2006; Wickramasinghe et al., 2008; Stritt and Knoll, 2010; Johnson et al., 2011; Lu and
402 Ramanan, 2011; Li et al., 2014). Deletion of SRF within neural stem cells specifically affected
403 differentiation to both astrocytes and oligodendrocytes (Lu and Ramanan, 2012). Interestingly,
404 neuronal SRF deletion did not affect astrocyte differentiation or cause any reactive astrogliosis
405 (Lu and Ramanan, 2012) but revealed a paracrine effect of neuronal SRF on oligodendrocyte
406 maturation and myelination (Stritt et al., 2009; Anastasiadou et al., 2015). Currently, the role of
407 SRF in astrocyte development remains poorly understood. This study identifies a critical role for
408 SRF in maintenance of astrocytes in a non-reactive state. However, it is possible that since SRF
409 deletion in the *Srf*^{GFAP}CKO mice likely starts around E16.5 during embryonic development, the
410 reactive astrogliosis could be due to developmental deficits.

411

412 Previous studies have shown that genetic ablation of the extracellular matrix protein, β 1-
413 integrin (Itg β 1) in astrocytes results in astrogliosis starting 4 weeks of age and Itg β 1 mutant mice
414 exhibit spontaneous seizures (Robel et al., 2009; Robel et al., 2015). Attenuation of sonic
415 hedgehog (Shh) signaling in postnatal astrocytes resulted in reactive astrocytes that were
416 restricted to the forebrain alone suggesting a role for Shh in maintaining the non-reactive state of
417 specific astrocytic populations (Garcia et al., 2010). Similarly, attenuation of fibroblast growth
418 factor (FGF) signaling by deletion of FGF receptors, FGFR1-3, resulted in astrogliosis that was

419 restricted to the neocortex and hippocampus although deletion occurred in other regions as well
420 (Kang et al., 2014b). Interestingly, expression of a dominant negative FGFR3 (dnFGFR3) and a
421 constitutively active FGFR3 (caFGFR3) in astrocytes produced different results. While
422 caFGFR3 suppressed astrogliosis in one study, it resulted in enlarged astrocytes with increased
423 branching in another (Kang et al., 2014a; Kang et al., 2014b). Furthermore, expression of a
424 dnFGFR3 suppressed GFAP expression and hypertrophic morphology (Kang et al., 2014a).
425 Nevertheless, these observations suggest an important role for FGF signaling in regulating the
426 reactive state of forebrain astrocytes. Since reactive astrocytes can either be beneficial or
427 detrimental to normal functioning of the nervous system, this process is expected to be tightly
428 regulated to maintain astrocytes in a non-reactive state.

429

430 Reactive astrocytes are induced or regulated by several extracellular signals including
431 cytokines, growth factors, endothelin, purines and lipopolysaccharide (LPS) and these factors are
432 released by neural and non-neural cells in the CNS following neuronal injury or in response to
433 infection (Kang and Hebert, 2011; Sofroniew, 2014). In the *Srf*^{GFAP}CKO mice, we did not
434 observe any cell death when analyzed at 2 weeks of age (Fig. 4A-C) and therefore, cell death is
435 unlikely to be the cause of gliosis, which was first observed starting at 3 weeks of age.
436 Furthermore, there were no discernible deficits observed in BBB permeability indicating that
437 reactive astrocytes in the *Srf* mutant mice are not induced by a leaky BBB (Fig. 5).

438

439 Depending on the severity of neural injury, astrogliosis can manifest as mild, moderate or
440 severe without or with scar formation (Pekny and Pekna, 2014; Sofroniew, 2014). During mild
441 and moderate astrogliosis, astrocytes exhibit hypertrophy, do not proliferate and return to non-

442 reactive state once the underlying cause is resolved (Pekny and Pekna, 2014; Sofroniew, 2014).
443 In severe astrogliosis, astrocytes exhibit proliferation and can also result in scar formation with
444 significant tissue rearrangement. In the *Srf*^{GFAP}CKO, the astrocytes exhibited hypertrophy but
445 were not proliferative when assessed in young and old mice (Fig. 4D, 6H). The absence of
446 proliferative hypertrophic reactive astrocytes has been reported in mutant mice carrying
447 astrocyte-specific deletion of genes such as Sonic hedgehog (Garcia et al., 2010), β 1-integrin
448 (Robel et al., 2009) and FGFR (Kang et al., 2014). Furthermore, the astrogliosis in these mutant
449 mice was found to be restricted to specific regions in the brain likely reflective of their
450 requirement in specific astrocyte populations. In contrast, in the *Srf* knockout mice, we observed
451 widespread astrogliosis in all regions of the brain including white matter astrocytes (Fig. 6A-G).
452 This suggests that conditional *Srf* ablation in astrocytes results in conversion to reactive
453 astrocytes irrespective of their regional heterogeneity (Zhang and Barres, 2010).

454

455 The *Srf* mutant mice also exhibited reactive microglia starting around 3 weeks of age and
456 persisted throughout adulthood (Fig. 7). Reactive astrogliosis has been shown to accompany
457 reactive microglia and vice versa (Frank and Wolburg, 1996; Zhang et al., 2010). Reactive
458 astrocytes are known to secrete cytokines, which can cause the activation of microglia (Davalos
459 et al., 2005). Since there appears to be no injury or infection in *Srf*^{GFAP}CKO mice, the microglial
460 activation is very likely to be caused by the reactive astrocytes.

461

462 Studies have shown that depending on the kind of neuronal injury or insult, reactive
463 astrocytes can be broadly classified as neurotoxic (A1) or neuroprotective (A2) (Li et al., 2008;
464 Zamanian et al., 2012; Liddelow et al., 2017). Since the SRF-deficient astrocytes exhibited

465 hypertrophy and enhanced GFAP and vimentin expression (Fig. 2, 3), we look at the expression
466 of A1 and A2 astrocyte markers. We found expression of more A2 marker genes as compared to
467 A1 genes in the brains Srf^{GFAP} CKO mice suggesting that SRF-deficient reactive astrocytes are
468 likely to be A2-type (Fig 8A). A1 reactive astrocytes have been shown to secrete neurotoxic
469 factor(s) that resulted in neuronal cell death in cultured neurons (Liddelow et al., 2017). The
470 presence of reactive microglia suggested that the reactive astrocytes could induce microgliosis.
471 We found an increased expression of $Il1\beta$ and $Ccl2/Mcp-1$ but not $Tnf\alpha$ in brains of
472 Srf^{GFAP} CKO mice (Fig. 8A). IL-1 β and the chemokine, CCL2/MCP-1 have been shown to
473 induce reactive microglia and could be the underlying cause for prolonged microgliosis (Selenica
474 et al., 2013; Liu and Quan, 2018). Since the Srf^{GFAP} CKO mice exhibited prolonged gliosis, we
475 analyzed for neuronal numbers and found no significant change in the number of neurons
476 indicating that the reactive astrocytes in the brains of these Srf mutant mice do not affect
477 neuronal survival (Fig. 8A-D).

478

479 In summary, we have identified SRF as a critical regulator of reactive astrocytes in the
480 mouse brain. Ablation of Srf in astrocyte-specific manner results in persistent and widespread
481 astrogliosis. Since astrocytes in all brain regions become reactive, it strongly suggests that SRF
482 is important for maintaining both white matter and grey matter astrocytes in a non-reactive state.
483 The SRF-deficient reactive astrocytes appear to be A2-like and the brains of Srf^{GFAP} CKO mice
484 exhibited normal neuronal numbers in spite of persistent gliosis. It is reasonable to speculate that
485 SRF expression needs to be downregulated for an astrocyte to become reactive. It is also
486 possible that SRF-dependent transcription is likely affected in reactive astrocytes observed in
487 neurodegenerative disorders. Future studies aimed at identification of SRF target genes may

488 provide novel insights into the mechanisms regulating reactive astrogliosis and may provide
489 potential targets for astrocyte-targeted therapeutics.

490 **REFERENCES**

- 491 Alberti S, Krause SM, Kretz O, Philippar U, Lemberger T, Casanova E, Wiebel FF, Schwarz H,
492 Frotscher M, Schutz G, Nordheim A (2005) Neuronal migration in the murine rostral migratory
493 stream requires serum response factor. *Proc Natl Acad Sci U S A* 102:6148-6153.
- 494 Andreone BJ, Chow BW, Tata A, Lacoste B, Ben-Zvi A, Bullock K, Deik AA, Ginty DD, Clish CB,
495 Gu C (2017) Blood-Brain Barrier Permeability Is Regulated by Lipid Transport-Dependent
496 Suppression of Caveolae-Mediated Transcytosis. *Neuron* 94:581-594 e585.
- 497 Bajenaru ML, Zhu Y, Hedrick NM, Donahoe J, Parada LF, Gutmann DH (2002) Astrocyte-
498 specific inactivation of the neurofibromatosis 1 gene (NF1) is insufficient for astrocytoma
499 formation. *Molecular and cellular biology* 22:5100-5113.
- 500 Barres BA (2008) The mystery and magic of glia: a perspective on their roles in health and
501 disease. *Neuron* 60:430-440.
- 502 Buffo A, Rite I, Tripathi P, Lepier A, Colak D, Horn AP, Mori T, Gotz M (2008) Origin and
503 progeny of reactive gliosis: A source of multipotent cells in the injured brain. *Proceedings of the*
504 *National Academy of Sciences of the United States of America* 105:3581-3586.
- 505 Burda JE, Sofroniew MV (2014) Reactive gliosis and the multicellular response to CNS damage
506 and disease. *Neuron* 81:229-248.
- 507 Correa-Cerro LS, Mandell JW (2007) Molecular mechanisms of astrogliosis: new approaches
508 with mouse genetics. *Journal of neuropathology and experimental neurology* 66:169-176.
- 509 Davalos D, Grutzendler J, Yang G, Kim JV, Zuo Y, Jung S, Littman DR, Dustin ML, Gan WB
510 (2005) ATP mediates rapid microglial response to local brain injury in vivo. *Nature neuroscience*
511 8:752-758.
- 512 Etkin A, Alarcon JM, Weisberg SP, Touzani K, Huang YY, Nordheim A, Kandel ER (2006) A role
513 in learning for SRF: deletion in the adult forebrain disrupts LTD and the formation of an
514 immediate memory of a novel context. *Neuron* 50:127-143.
- 515 Frank M, Wolburg H (1996) Cellular reactions at the lesion site after crushing of the rat optic
516 nerve. *Glia* 16:227-240.
- 517 Garcia AD, Petrova R, Eng L, Joyner AL (2010) Sonic hedgehog regulates discrete populations
518 of astrocytes in the adult mouse forebrain. *The Journal of neuroscience : the official journal of*
519 *the Society for Neuroscience* 30:13597-13608.
- 520 Johnson AW, Crombag HS, Smith DR, Ramanan N (2011) Effects of serum response factor
521 (SRF) deletion on conditioned reinforcement. *Behav Brain Res* 220:312-318.

- 522 Kang W, Hebert JM (2011) Signaling pathways in reactive astrocytes, a genetic perspective.
523 *Molecular neurobiology* 43:147-154.
- 524 Kang W, Balordi F, Su N, Chen L, Fishell G, Hebert JM (2014) Astrocyte activation is
525 suppressed in both normal and injured brain by FGF signaling. *Proceedings of the National*
526 *Academy of Sciences of the United States of America* 111:E2987-2995.
- 527 Kimelberg HK (2010) Functions of mature mammalian astrocytes: a current view. *Neuroscientist*
528 16:79-106.
- 529 Kimelberg HK, Nedergaard M (2010) Functions of astrocytes and their potential as therapeutic
530 targets. *Neurotherapeutics* 7:338-353.
- 531 Knoll B, Nordheim A (2009) Functional versatility of transcription factors in the nervous system:
532 the SRF paradigm. *Trends Neurosci* 32:432-442.
- 533 Knoll B, Kretz O, Fiedler C, Alberti S, Schutz G, Frotscher M, Nordheim A (2006) Serum
534 response factor controls neuronal circuit assembly in the hippocampus. *Nat Neurosci* 9:195-
535 204.
- 536 Li CL, Sathyamurthy A, Oldenburg A, Tank D, Ramanan N (2014) SRF phosphorylation by
537 glycogen synthase kinase-3 promotes axon growth in hippocampal neurons. *J Neurosci*
538 34:4027-4042.
- 539 Li L et al. (2008) Protective role of reactive astrocytes in brain ischemia. *Journal of cerebral*
540 *blood flow and metabolism : official journal of the International Society of Cerebral Blood Flow*
541 *and Metabolism* 28:468-481.
- 542 Liddelow SA, Barres BA (2017) Reactive Astrocytes: Production, Function, and Therapeutic
543 Potential. *Immunity* 46:957-967.
- 544 Liddelow SA et al. (2017) Neurotoxic reactive astrocytes are induced by activated microglia.
545 *Nature* 541:481-487.
- 546 Liu X, Quan N (2018) Microglia and CNS Interleukin-1: Beyond Immunological Concepts. *Front*
547 *Neurol* 9:8.
- 548 Lu PP, Ramanan N (2011) Serum response factor is required for cortical axon growth but is
549 dispensable for neurogenesis and neocortical lamination. *J Neurosci* 31:16651-16664.
- 550 Lu PP, Ramanan N (2012) A critical cell-intrinsic role for serum response factor in glial
551 specification in the CNS. *J Neurosci* 32:8012-8023.
- 552 Pekny M, Nilsson M (2005) Astrocyte activation and reactive gliosis. *Glia* 50:427-434.
- 553 Pekny M, Pekna M (2014) Astrocyte reactivity and reactive astrogliosis: costs and benefits.
554 *Physiological reviews* 94:1077-1098.

- 555 Phatnani H, Maniatis T (2015) Astrocytes in neurodegenerative disease. Cold Spring Harbor
556 perspectives in biology 7.
- 557 Ramanan N, Shen Y, Sarsfield S, Lemberger T, Schutz G, Linden DJ, Ginty DD (2005) SRF
558 mediates activity-induced gene expression and synaptic plasticity but not neuronal viability. Nat
559 Neurosci 8:759-767.
- 560 Ridet JL, Malhotra SK, Privat A, Gage FH (1997) Reactive astrocytes: cellular and molecular
561 cues to biological function. Trends in neurosciences 20:570-577.
- 562 Robel S, Mori T, Zoubaa S, Schlegel J, Sirko S, Faissner A, Goebbels S, Dimou L, Gotz M
563 (2009) Conditional deletion of beta1-integrin in astroglia causes partial reactive gliosis. Glia
564 57:1630-1647.
- 565 Seifert G, Schilling K, Steinhauser C (2006) Astrocyte dysfunction in neurological disorders: a
566 molecular perspective. Nat Rev Neurosci 7:194-206.
- 567 Selenica ML, Alvarez JA, Nash KR, Lee DC, Cao C, Lin X, Reid P, Mouton PR, Morgan D,
568 Gordon MN (2013) Diverse activation of microglia by chemokine (C-C motif) ligand 2
569 overexpression in brain. Journal of neuroinflammation 10:86.
- 570 Sofroniew MV (2005) Reactive astrocytes in neural repair and protection. The Neuroscientist : a
571 review journal bringing neurobiology, neurology and psychiatry 11:400-407.
- 572 Sofroniew MV (2009) Molecular dissection of reactive astrogliosis and glial scar formation.
573 Trends in neurosciences 32:638-647.
- 574 Sofroniew MV (2014) Astrogliosis. Cold Spring Harbor perspectives in biology 7:a020420.
- 575 Sofroniew MV (2015) Astrocyte barriers to neurotoxic inflammation. Nature reviews
576 Neuroscience 16:249-263.
- 577 Stritt C, Knoll B (2010) Serum response factor regulates hippocampal lamination and dendrite
578 development and is connected with reelin signaling. Mol Cell Biol 30:1828-1837.
- 579 Stritt C, Stern S, Harting K, Manke T, Sinske D, Schwarz H, Vingron M, Nordheim A, Knoll B
580 (2009) Paracrine control of oligodendrocyte differentiation by SRF-directed neuronal gene
581 expression. Nat Neurosci 12:418-427.
- 582 Wickramasinghe SR, Alvania RS, Ramanan N, Wood JN, Mandai K, Ginty DD (2008) Serum
583 response factor mediates NGF-dependent target innervation by embryonic DRG sensory
584 neurons. Neuron 58:532-545.
- 585 Zamanian JL, Xu L, Foo LC, Nouri N, Zhou L, Giffard RG, Barres BA (2012) Genomic analysis
586 of reactive astrogliosis. The Journal of neuroscience : the official journal of the Society for
587 Neuroscience 32:6391-6410.

- 588 Zhang D, Hu X, Qian L, O'Callaghan JP, Hong JS (2010) Astrogliosis in CNS pathologies: is
589 there a role for microglia? *Molecular neurobiology* 41:232-241.
- 590 Zhang Y, Barres BA (2010) Astrocyte heterogeneity: an underappreciated topic in neurobiology.
591 *Curr Opin Neurobiol* 20:588-594.
- 592

593 **FIGURE LEGENDS**

594

595 **Figure 1.** Astrocyte-specific deletion of *Srf* in *Srf*^{GFAP}CKO mice. (A) Representative images of
596 immunostaining for SRF (red), S100 β (green) and NeuN (blue) shows SRF expression in
597 astrocytes (arrows) and neurons (arrowheads) in the cortex and striatum of control mice. SRF
598 expression was seen only in the neurons but not in the astrocytes in *Srf*^{GFAP}CKO mice mutant
599 mice. A' shows representative higher magnification images of astrocytes and neurons from (A)
600 showing SRF expression in control astrocytes and neurons, and absent in mutant astrocytes. (B)
601 Quantification of SRF immunofluorescence in S100 β + astrocytes from (A). At least 15-20 cells
602 per mouse were analyzed (n=3 mice). Astrocytes: cortex, control (16.49 \pm 2.52), *Srf*^{GFAP}CKO
603 (4.80 \pm 0.29); Striatum, control (19.72 \pm 3.179), *Srf*^{GFAP}CKO (7.40 \pm 1.47); Neurons: cortex, control
604 (24.33 \pm 5.05), *Srf*^{GFAP}CKO, control (28.47 \pm 5.60); Striatum, control (30.79 \pm 1.40), *Srf*^{GFAP}CKO
605 (23.41 \pm 3.09). (C) Quantitative real time PCR from whole brain total RNA shows a significant
606 decrease in *Srf* mRNA expression in the mutant mice relative to control mice; Control (1.0 \pm 0),
607 *Srf*^{GFAP}CKO (0.30 \pm 0.14) (n=3 mice). (D) Semi-quantitative PCR from whole brain total RNA
608 shows a significant decrease in *Srf* mRNA expression in the mutant mice. *Rps29* expression
609 served as the loading control (n=3 mice). Control (1.04 \pm 0.01), *Srf*^{GFAP}CKO (0.24 \pm 0.02) (n=3
610 mice). Scale bars, 50 μ m (A), 20 μ m (A'). ** P < 0.005, *** P < 0.0005, **** P < 0.0001, ns,
611 not significant. Two tailed t-test. Data are mean \pm SEM.

612

613 **Figure 2.** Conditional deletion of SRF in astrocytes results in reactive gliosis. (A) Representative
614 images of immunostaining for GFAP and ALDH1L1 in 3-wk old *Srf*^{GFAP}CKO and control
615 littermates shows higher expression of these markers in neocortex (Ctx) and hippocampus (Hc)

616 of mutant mice as compared to control littermates. **(B, C)** GFAP and S100 β immunostaining
617 also showed that the astrocytes in mutant mice were hypertrophic compared to control mice,
618 (n=3 mice). **(D)** Quantification of S100 β ⁺ astrocytes from (C). Cortex, control (76.58 \pm 1.19),
619 *Srf*^{GFAP}CKO (50.25 \pm 5.67); Striatum, control (70.71 \pm 3.61), *Srf*^{GFAP}CKO (66.04 \pm 3.72);
620 Hippocampus, control (11.90 \pm 0.17), *Srf*^{GFAP}CKO (10.88 \pm 1.14) (n=3 mice). Scale bars, 100 μ m
621 **(A)**, 50 μ m **(B, C)**; ns, not significant. Two tailed *t*-test. Data are mean \pm SEM.

622

623 **Figure 3.** SRF ablation in astrocytes leads to widespread astrogliosis. **(A)** Representative images
624 of immunostaining for the astrogliosis marker, nestin in 3-wk old *Srf*^{GFAP}CKO and control
625 littermates shows reactive astrocytes in cortex and hippocampus of *Srf* mutant mice but not in
626 control littermates. **(B)** Quantification of nestin fluorescence intensity shown in (A). Cortex:
627 control (0.0 \pm 0.14), *Srf*^{GFAP}CKO (771.9 \pm 16.14), hippocampus: control (0.0 \pm 8.15), *Srf*^{GFAP}CKO
628 (556.1 \pm 38.56) (n=3 mice). **(C)** Representative images showing co-immunostaining with GFAP
629 and the gliosis marker, vimentin. There is little or no GFAP and vimentin expression in 3-wk
630 control mice. In contrast, the astrocytes in mutant mice exhibit strong expression and
631 colocalization of GFAP and vimentin. **(D)** Quantification of fluorescence intensity in (C). For
632 GFAP, cortex, control (102.1 \pm 5.28), *Srf*^{GFAP}CKO (580.1 \pm 62.10); hippocampus, control
633 (228.0 \pm 34.20), *Srf*^{GFAP}CKO (638.1 \pm 73.97); striatum, control (85.78 \pm 1.83), *Srf*^{GFAP}CKO
634 (256.9 \pm 7.73); For vimentin, cortex, control (2.93 \pm 0.99), *Srf*^{GFAP}CKO (674.10 \pm 27.70);
635 hippocampus, control (12.02 \pm 12.02), *Srf*^{GFAP}CKO (964.10 \pm 11.79); striatum, control (2.33 \pm 0.33),
636 *Srf*^{GFAP}CKO (633.50 \pm 41.37). Shown here are neocortex, hippocampus (Hpc) and striatum (Str)
637 (n=3 mice). Scale bar, 500 μ m **(A)**, 50 μ m **(C)**. ** P < 0.005, *** P < 0.0005, **** P < 0.0001,
638 Two tailed *t*-test. Data are mean \pm SEM.

639

640 **Figure 4.** Absence of cell death in *Srf* mutant mice. **(A)** Representative images of TUNEL
641 staining of 2-wk old *Srf*^{GFAP}CKO mice and control littermates. Amplified view of boxed region
642 is shown on right. Arrows show TUNEL⁺ cells while the arrowhead shows non-specific
643 staining. **(B)** Representative images of immunostaining for cleaved caspase-3 in the neocortex
644 and hippocampus of 2-wk old *Srf*^{GFAP}CKO mice and control littermates. Amplified view of
645 boxed region is shown on right. Arrows show TUNEL⁺ cells while the arrowhead shows non-
646 specific staining. **(C)** Quantification of TUNEL⁺ and cleaved Caspase-3⁺ cells in neocortex and
647 hippocampus shows the no significant difference in the number of dead cells between
648 *Srf*^{GFAP}CKO mice and control littermates. Caspase-3: cortex, control (2.20±1.00), *Srf*^{GFAP}CKO
649 (1.45±0.77); hippocampus, control, (1.16±0.65), *Srf*^{GFAP}CKO (0.91±0.79). TUNEL: cortex,
650 control (0.37±0.21), *Srf*^{GFAP}CKO (0.08±0.052); hippocampus, control (0.81±0.21), *Srf*^{GFAP}CKO
651 (1.18± 0.25) (n=3 mice). **(D)** Representative images of immunostaining for the proliferation
652 marker, phosphohistone H3 (phH3) in 3-wk old *Srf*^{GFAP}CKO and their respective control mice
653 showed no proliferating cells in the mutant mice. Immunostaining of P0.5 mouse brain section
654 showed many phH3-positive cells and served as a control. n.s, not significant. Two-tailed t-test.
655 Data are mean ± SEM. Scale bar, 20 μm (**A'**, **B'**) and 200 μm; (n=3 mice).

656

657 **Figure 5.** Blood brain barrier is not compromised in *Srf*^{GFAP}CKO mice. **(A)** Schematic diagram
658 showing experimental timeline of dextran fluorescein and HRP injection and tissue processing.
659 **(B)** 10 kDa TMR-Dextran (Dextran fluorescein, DF) tracer injection reveals normal architecture
660 of cerebral vasculature in 3- to 5-wk old *Srf*^{GFAP}CKO and their control littermates. **(C)**
661 Quantification of ratio of fluorescence intensity outside vs inside the blood vessel reveals no

662 significant difference between Srf^{GFAP} CKO mice and their control littermates, indicative of intact
663 blood brain barrier. A stab-wounded brain served as a control to show BBB leakage. Control
664 (0.21 ± 0.0), Srf^{GFAP} CKO (0.18 ± 0.05), Stab-wound (1.97 ± 0.26) (n=3 mice). (D) Transcardial
665 injection of 44 kDa HRP type II in Srf^{GFAP} CKO mice and their respective controls, shows that
666 HRP was restricted to the blood vessel lumen. (E) Quantification of ratio of color intensity
667 outside vs inside the blood vessel shows no significant difference between control and mutant
668 mice (n=3 mice). Control (0.16 ± 0.05), Srf^{GFAP} CKO (0.20 ± 0.02), Stab-wound (1.45 ± 0.08) (n=3
669 mice). Scale bar, 400 μ m (B), 200 μ m (D). ns, not significant. **** P < 0.0001, one-way
670 ANOVA, data are mean \pm SD.

671

672 **Figure 6.** Persistent astrogliosis in Srf^{GFAP} CKO mice. (A) Immunostaining for GFAP in 3-
673 month old Srf^{GFAP} CKO mice and control littermates shows widespread astrogliosis in all the
674 brain regions. (B) Quantification of color intensity in (A). Cortex, control (107.2 ± 0.61),
675 Srf^{GFAP} CKO (176.4 ± 7.35); hippocampus, control (270.2 ± 9.11), Srf^{GFAP} CKO (385.4 ± 16.14);
676 striatum, control (151.4 ± 1.280), Srf^{GFAP} CKO (260.6 ± 18.58) (n=3 mice). (C) Representative
677 images of immunostaining for GFAP in 12-month old Srf^{GFAP} CKO mice and control littermates
678 shows persistent astrogliosis in all the brain regions analyzed. Shown here are cortex,
679 hippocampus (Hpc) and striatum. (D) Quantification of relative color intensity in (C).
680 Quantification of color intensity in (C); cortex, control (188.2 ± 2.85), Srf^{GFAP} CKO
681 (536.0 ± 26.03); hippocampus, control (356.3 ± 6.89), Srf^{GFAP} CKO (591.0 ± 29.43); striatum: control
682 (191.1 ± 4.83), Srf^{GFAP} CKO (495.7 ± 80.51) (n=3 mice). (E) Representative images of
683 immunostaining for reactive astrogliosis marker, vimentin, in 3-mon and 12-mon old
684 Srf^{GFAP} CKO mice and control littermates shows gliosis astrocytes only in the brains of Srf

685 mutant mice. **(F, G)** Relative fluorescent intensity of vimentin immunostaining in 3-month (F)
686 and 12-month (G) old mice compared to control littermates. (F) Cortex, control, (11.52±11.52),
687 $Srf^{GFAP}CKO$ (317.1±39.27); hippocampus: control (4.47±3.11), $Srf^{GFAP}CKO$ (378.7±8.17),
688 striatum: control (5.43±5.43), $Srf^{GFAP}CKO$ (110.8±4.94). (G) Cortex, control (8.22±4.11),
689 $Srf^{GFAP}CKO$ (475.7±67.75); hippocampus, control (10.26±10.26), $Srf^{GFAP}CKO$ (531.6±31.96);
690 striatum: control (17.30±11.98), $Srf^{GFAP}CKO$ (157.4±13.96) (n=3-4 mice). **(H)** Immunostaining
691 for the proliferation marker, phosphohistone H3 (pH3) in 12-month old $Srf^{GFAP}CKO$ and
692 control littermates showed no proliferating cells even at this age. Scale bar, 200 μ m. * P < 0.05,
693 ** P < 0.005, *** P < 0.0005, **** P < 0.0001, Two tailed *t*-test. Data are mean \pm SEM.

694

695 **Figure 7.** Microglial activation is seen along with astrogliosis in $Srf^{GFAP}CKO$ mice. **(A)**
696 Immunostaining for the microglia marker, Iba1 showed increased Iba1 expression in the
697 neocortex and hippocampus of mutant mice as compared to the control littermates, suggesting
698 activated microglia in mutant brain. **(B)** Relative fluorescence intensity of Iba1 in the neocortex
699 of Srf mutant mice compared to control littermates in (A) shows a significant increase in Iba1
700 expression in the Srf mutants indicative of microgliosis. Control (1.0±0.0), $Srf^{GFAP}CKO$
701 (1.97±0.19) (n=3 mice). **(C)** Quantification of Iba1⁺ cells in 3-wk old control and mutant mice.
702 Cortex, control (29.08±0.43), $Srf^{GFAP}CKO$ (34.4±2.68); hippocampus (Hpc), control
703 (28.64±0.82), $Srf^{GFAP}CKO$ (33.80±1.40); striatum, control (29.46±1.20), $Srf^{GFAP}CKO$
704 (32.0±0.42) (n=3 mice). **(D)** Representative images of sections immunostained for microglial
705 marker Iba1 in aged mice (3-month and 12-month old) in $Srf^{GFAP}CKO$ and control littermates
706 show increased expression of Iba1 in the Srf mutants. Shown here is neocortex. **(E)** Relative
707 fluorescence intensity of Iba1 in the neocortex of Srf mutant mice compared to control

708 littermates shows persistent microgliosis in the *Srf* mutants throughout adulthood. 3 mon, control
 709 (1.0±0.0), *Srf*^{GFAP}CKO (1.8±0.22); 12 mon, Control (1.0±0.0), *Srf*^{GFAP}CKO (1.71±0.17) (n=3
 710 mice). **(F, G)** Quantification of Iba1⁺ cells at 3 mon (F), cortex, control (30.00±0.62),
 711 *Srf*^{GFAP}CKO (54.50±6.87); hippocampus (Hpc), control (24.00±4.25), *Srf*^{GFAP}CKO (58.75±9.00);
 712 striatum, control (29.25±1.25), *Srf*^{GFAP}CKO (32.75±3.00); and 12 mon (G) cortex, control
 713 (28.25±0.57), *Srf*^{GFAP}CKO (38.75±2.49); hippocampus, control (27.58±1.55), *Srf*^{GFAP}CKO
 714 (36.75±6.00); striatum, control (28.17±0.88), *Srf*^{GFAP}CKO (28.58±1.17). (n=3 mice), Scale bars,
 715 200 μm; ** P < 0.005. ns, not significant. Two tailed t-test. Data are mean ± SEM.

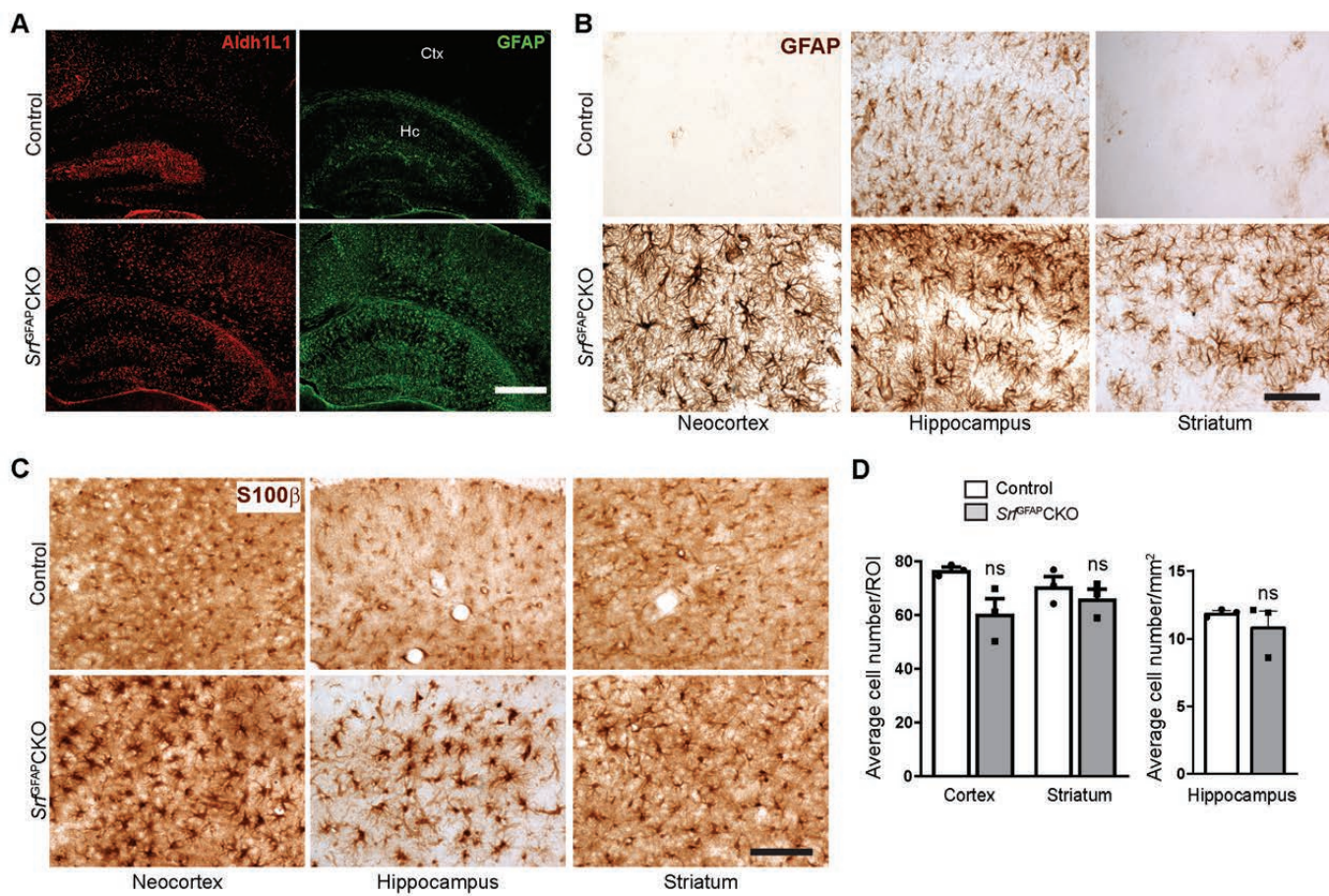
716

717 **Figure 8.** Prolonged gliosis in *Srf*^{GFAP}CKO mice does not affect neuronal survival. **(A)**
 718 Quantitative realtime PCR for A1, A2, pan reactive astrocyte markers and neuroinflammatory
 719 genes shows expression of a greater number of A2 reactive genes in the brains of *Srf* mutant
 720 mice compared to A1 genes. The mutant astrocytes also exhibited a higher expression of
 721 neuroinflammatory genes, *Il1β* and *Ccl2/Mcp-1* but not *TNFα*. Control (1.0±0.0), *Srf*^{GFAP}CKO,
 722 *Cd109* (3.49±0.62), *Ccl1* (2.51±0.52), *Cd14* (2.82±0.51), *Ptgs2* (0.90±0.25), *Psm8*
 723 (7.43±0.83), *H2T23* (2.20±0.78), *H2D1* (2.4±0.65), *Srgn* (1.78±0.39), *Serpina3n* (10.88±1.86),
 724 *Gfap* (9.62±0.84), *Il1β* (1.806±0.16), *Ccl2/Mcp-1*(13.52±1.967), *TNFα* (3.35±0.97) (n=3 mice).
 725 **(B)** Representative images of immunostaining for the neuronal marker, NeuN shows normal
 726 structural integrity in 3-5 wk old *Srf*^{GFAP}CKO mice compared to control littermates. **(C, D)**
 727 Quantification of NeuN⁺ cells in 3-5 wk old (C) and 12-mon old (D) control and mutant mice
 728 shows no significant change in neuronal numbers in the mutant mice. (C) cortex, control
 729 (209.5±12.10), *Srf*^{GFAP}CKO (195.2±11.18); CA1, control (78.25±16.48), *Srf*^{GFAP}CKO
 730 (148.4±34.10); CA3, control (124.4±24.47), *Srf*^{GFAP}CKO (133.5±37.20); striatum, control

731 (220.8±5.90), Srf^{GFAP} CKO (205.8±19.59) (n=3 mice). (D) cortex, control (208.4±9.87),
732 Srf^{GFAP} CKO (190.0±9.71); CA1, control (119.0±22.36), Srf^{GFAP} CKO (148.2±12.23); CA3,
733 control (101.0±22.05), Srf^{GFAP} CKO (127.8±12.19); striatum, control (211.1±5.14), Srf^{GFAP} CKO
734 (182.1±51.89) (n=3 mice), Scale bar, 1 mm; * P < 0.05, ** P < 0.005, *** P < 0.0005, ns, not
735 significant. Two tailed t-test. Data are mean ± SEM.

736

Figure 2



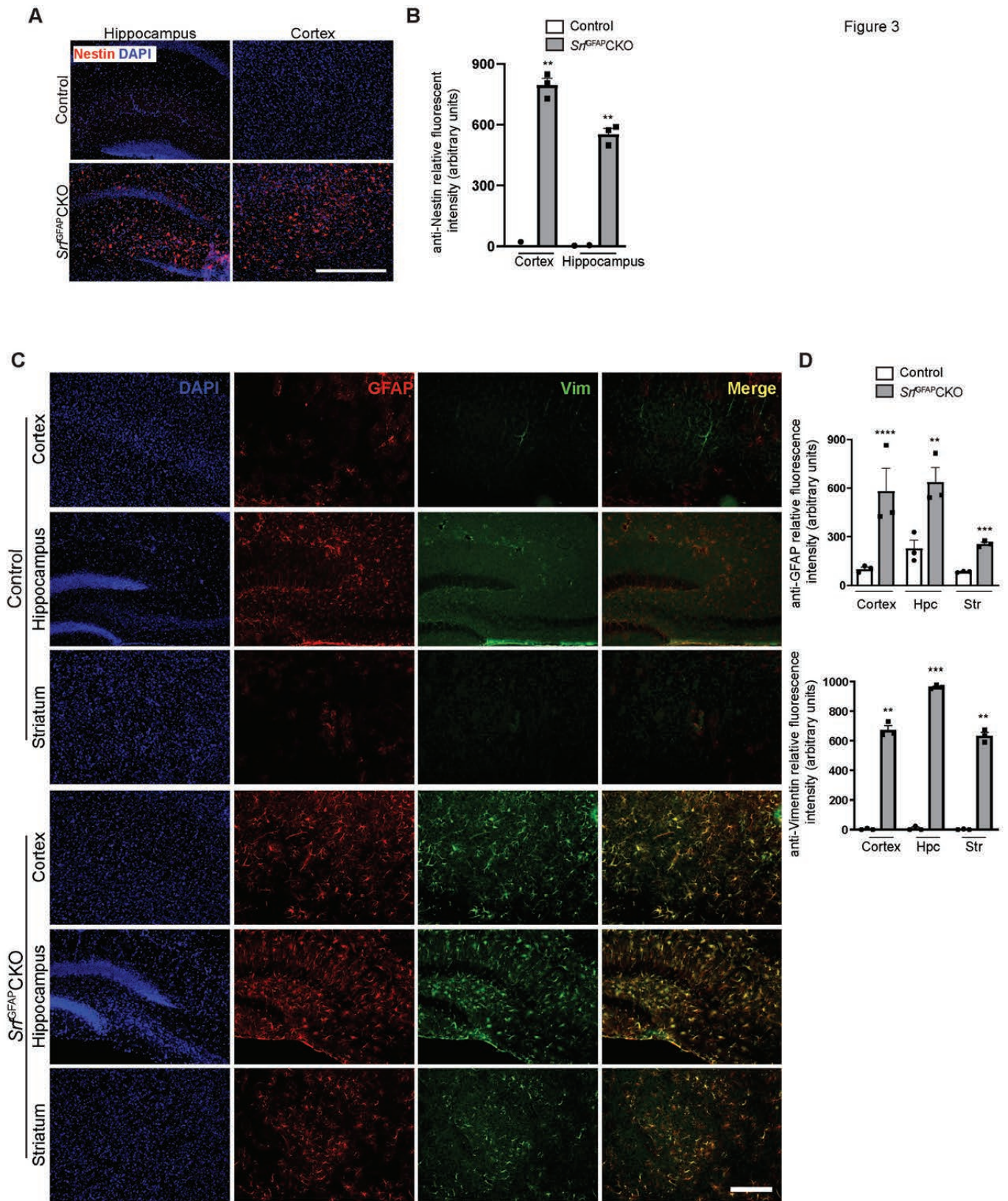


Figure 3

Figure 4

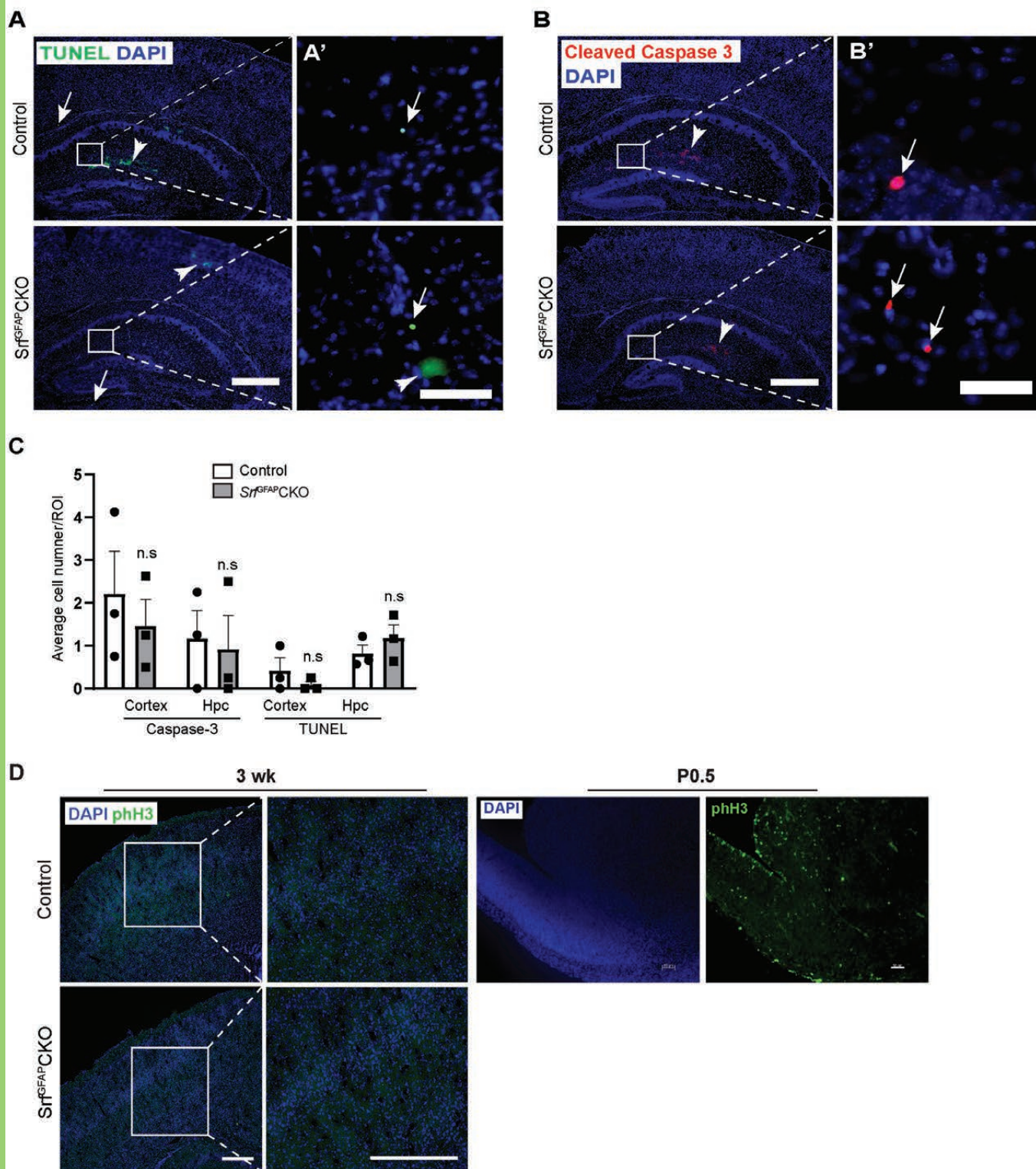


Figure 5

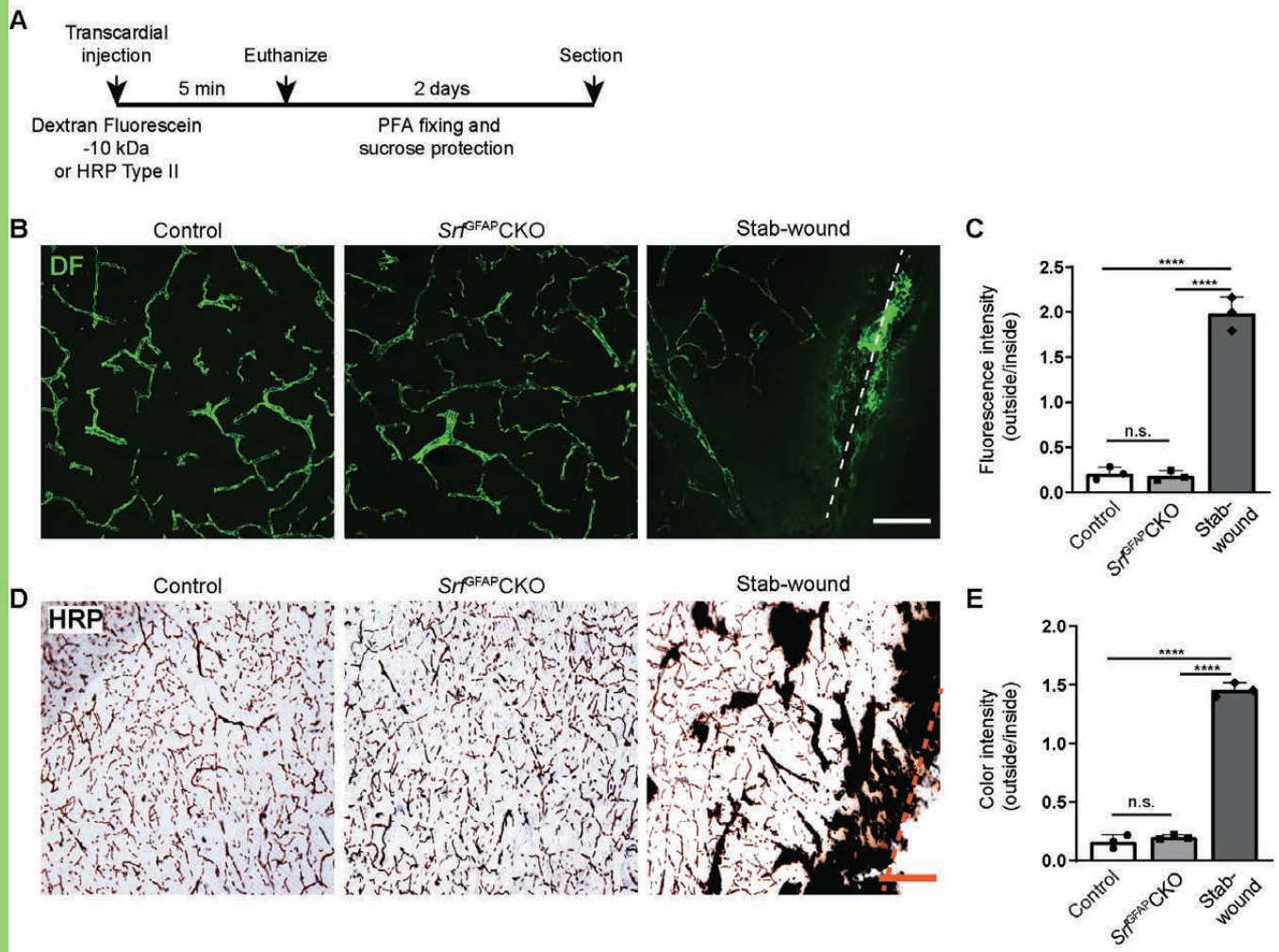


Figure 6

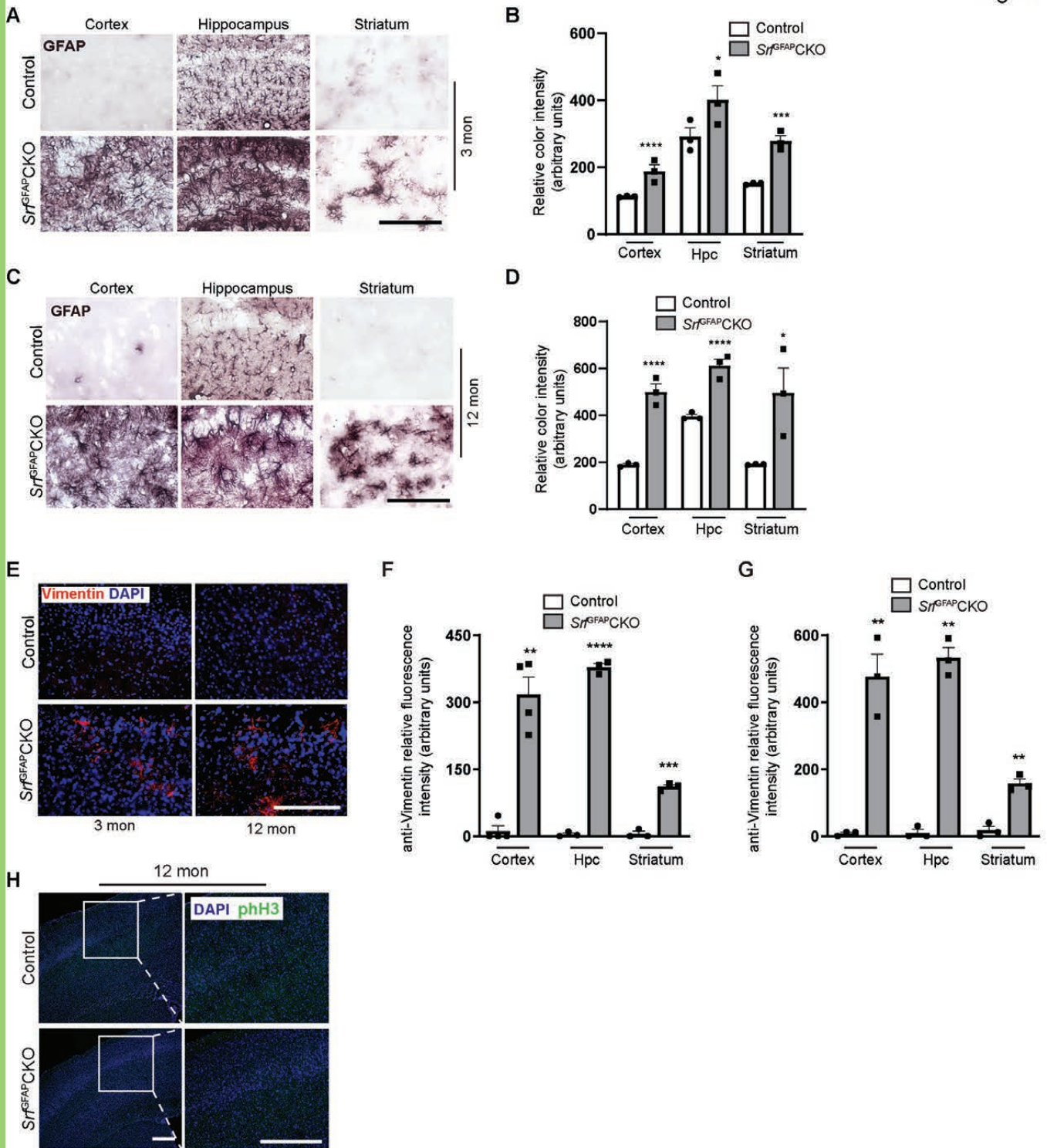


Figure 7

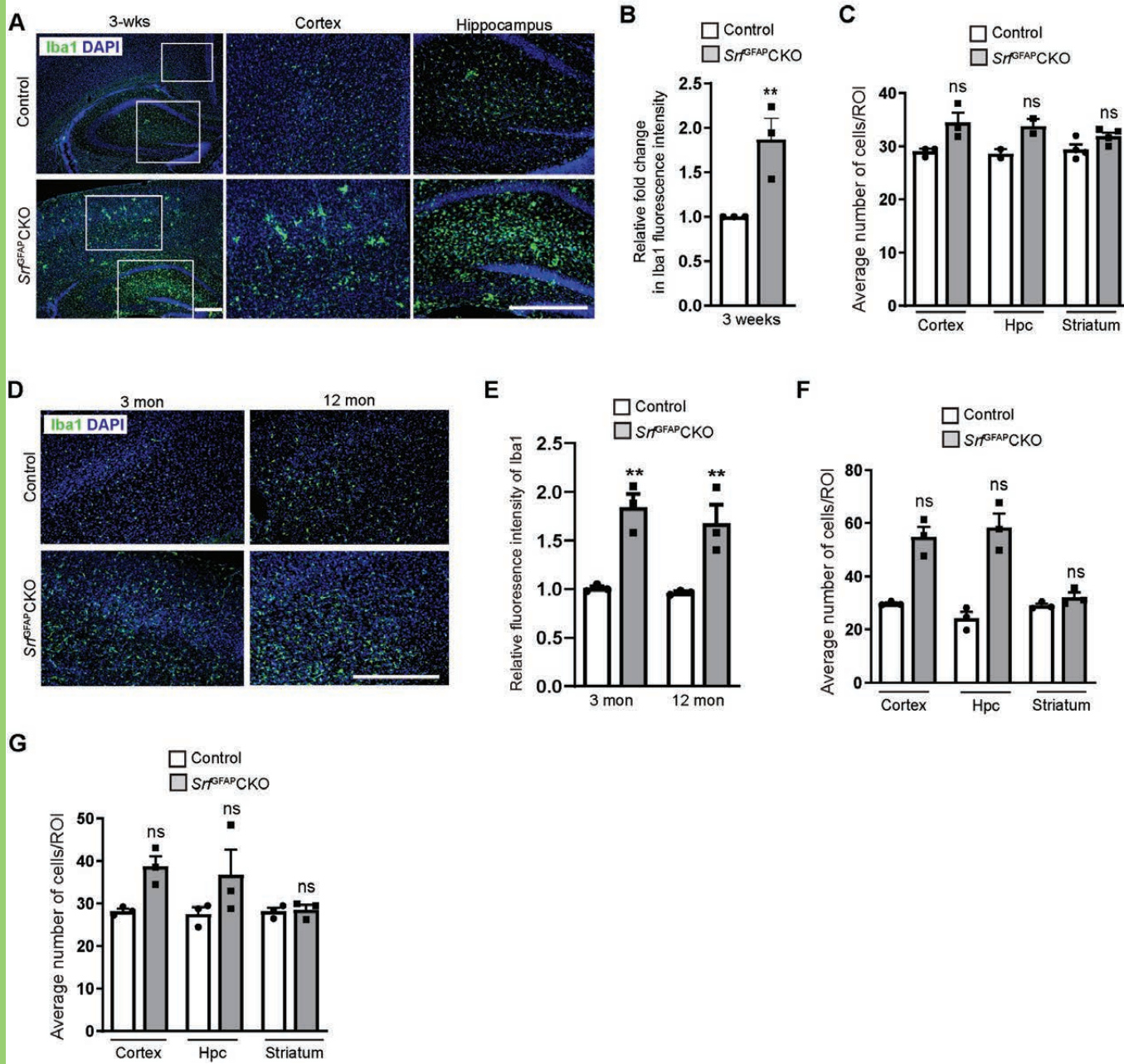


Figure 8

